

Particle interactions in colloidal aggregation by Brownian dynamics simulation

A. M. Puertas,¹ J. A. Maroto,² A. Fernández Barbero,¹ and F. J. de las Nieves^{1,*}

¹Group of Complex Fluids Physics, Department of Applied Physics, University of Almería, 04120 Almería, Spain

²Department of Applied Physics, University of Jaén, 23700 Linares, Jaén, Spain

(Received 10 August 1998)

We perform a Brownian dynamics simulation for describing the first stages of cluster formation. Special attention has been paid to systems composed of particles of opposite charges. Results are compared with light scattering experiments, obtaining a very good agreement, which validates the simulation model.

[S1063-651X(99)02402-2]

PACS number(s): 82.70.Dd

I. INTRODUCTION

Colloidal particle aggregation has proven to be reasonably well described by the von Smoluchowski kinetics based on mean field approximations [1–4]. However, when some asymmetries are introduced in the system such as size polydispersity or differences in particle charges, the description becomes more complex. Dissimilar particle aggregation processes are referred to as heteroaggregation. Special attention is focused on the aggregation of particles bearing opposite charge sign [5–10].

Simulation based on the control of particle sticking reproduces fairly well the diffusion limited aggregation for which the probability is one, and the reaction velocity is only determined by the diffusion of particles. Also, reaction limited processes are properly described with sticking probabilities lower than one [11–13]. In the case of heteroaggregation, models based on sticking probabilities cannot be used for describing reactions that may be faster than diffusion controlled, due to attraction between particles. In this sense, simulation based on a direct calculation of the interactions must be employed. This fact encourages the use of Brownian dynamics as the most appropriate model for simulating such situations. Brownian dynamics has been successfully applied recently for systems where the particle interactions play a determinant role [14–16].

In this work, heteroaggregation of particles with opposite charges has been studied at short aggregation times, for which only dimer formation is occurring. A particle-particle Brownian dynamics simulation has been performed. A cross-over between processes dominated by attraction forces to diffusion controlled aggregations was found. Acceptable results were obtained, as comparison with light scattering experiment demonstrates.

II. THEORY

The interaction of a spherical Brownian particle with the solvent molecules can be separated into two parts [17]: (i) a rapidly varying force $\vec{f}(t)$ resulting from random collisions of the solvent molecules with the particle, and (ii) a frictional force \vec{F}_f due to systematic collisions with the solvent mol-

ecules as the particle moves, which depends on the particle velocity. Therefore, the resulting Newton's equation governing the particle motion is

$$\frac{d\vec{p}}{dt} = -\vec{F}_f + \vec{f}, \quad (1)$$

which is known as the Langevin equation. For low Reynolds number, the friction force is described by Stokes' law:

$$\vec{F}_f(\vec{p}) = 6\pi a \eta \vec{v} = \gamma \frac{\vec{p}}{M}, \quad (2)$$

where η is the medium viscosity, γ is the friction coefficient, and a the particle radius. Nevertheless, for the fluctuating force $\vec{f}(t)$, there is no expression available. Only, some properties are known: its temporal average is zero, and it is δ correlated:

$$\langle \vec{f}(t) \rangle = 0 \quad \langle \vec{f}(t) \vec{f}(t') \rangle = \bar{G} \delta(t-t'), \quad (3)$$

where \bar{G} is a constant 3×3 dimensional tensor, referred to as the fluctuation strength.

Equation (1) can be solved both in $\vec{p}(t)$ and $\vec{r}(t)$. The use of these solutions within Chandrasekhar's theorem for random path [17,18], allows the probability density function (PDF), to be evaluated. This provides the probability of finding the particle at position \vec{r} , in time t , given that it was in \vec{r}_0 at time t_0 :

$$P(\vec{r}, t | \vec{r}_0, t_0) = \frac{1}{(4\pi D_0 \Delta t)^{3/2}} \exp \left\{ - \frac{\left| \vec{r} - \vec{r}_0 - \frac{\vec{p}_0}{\gamma} \right|^2}{4D_0 \Delta t} \right\}, \quad (4)$$

where D_0 is the diffusion coefficient, defined as $D_0 = k_B T / 6\pi \eta a$, with k_B the Boltzmann constant and T the temperature. This PDF is Gaussian shaped, with the maximum located at the position the particle would take in absence of diffusion.

The time scale has to be larger than the interaction between the Brownian particle and the solvent molecules time scale, to validate features in Eq. (3). The smallest time scale on which the above conditions can be applied is referred to as the Fokker-Planck time scale, τ_{FP} . On the other hand, the

*Author to whom correspondence should be addressed.

momentum of the particle relaxes to zero on a time scale larger than $M/\gamma \sim 10^{-9}$ s; and thus recovers equilibrium with the solvent molecules. Therefore, the time scale we are interested in, which is much larger than the Fokker-Planck time scale, and also larger than M/γ , will be referred to as diffusive or Brownian time scale τ_D . Thus, the ordering of time scales is

$$\tau_{\text{solvent}} \ll \tau_{\text{FP}} \ll M/\gamma \ll \tau_D.$$

Since the particle momentum relaxes to zero, the corresponding term in Eq. (4) can be eliminated, resulting in

$$P(\vec{r}, t | \vec{r}_0, t_0) = \frac{1}{(4\pi D_0 \Delta t)^{3/2}} \exp\left\{-\frac{|\vec{r} - \vec{r}_0|^2}{4D_0 \Delta t}\right\}. \quad (5)$$

When external forces \vec{F}_{ext} act on the particle, a new term must be included in the Langevin equation:

$$\frac{d\vec{p}}{dt} = -\vec{F}_f(\vec{p}) + \vec{f}(t) + \vec{F}_{\text{ext}}. \quad (6)$$

This equation is solvable, for constant \vec{F}_{ext} and using Eqs. (2) and (3). Finally, the PDF in the diffusive time scale is

$$P(\vec{r}, t | \vec{r}_0, t_0) = \frac{1}{(4\pi D_0 \Delta t)^{3/2}} \exp\left\{-\frac{\left|\vec{r} - \vec{r}_0 - \frac{\vec{F}_{\text{ext}} \Delta t}{\gamma}\right|^2}{4D_0 \Delta t}\right\}. \quad (7)$$

III. MODEL

Using Eq. (7), a random path for a particle submitted in an external field is performed. The new particle position after a small time, Δt , will be considered as initial position for the next step, this procedure being repeated for every step. A Box-Muller algorithm has been employed to generate random numbers according to a Gaussian distribution [19,20].

Interactions between particles have to be taken into account by means of the force exerted on one particle. However, forces are not constant, since they depend on the interparticle distance. This requirement in the evaluation of Eq. (7) can be overcome by considering a sufficiently small time step, Δt , for which position changes are not excessively large and the force may be considered as constant. Thus, application of Eq. (7) must be restricted to small time steps, but larger than M/γ as discussed in the previous section.

In this work, the interaction force between particles has been obtained by superposition of London-van der Waals attraction and electrostatic interaction, as proposed by Derjaguin and Landau [21] and Verwey and Overbeek [22] (DLVO theory). The expressions derived by Hogg, Healy, and Fuerstenau (HHF) [23] for those interactions, corresponding to dissimilar particles have been used:

$$V_A(r) = -\frac{A}{6} \left\{ \frac{2a_1 a_2}{r^2 - (a_1 + a_2)^2} + \frac{2a_1 a_2}{r^2 - (a_1 - a_2)^2} + \ln \frac{r^2 - (a_1 + a_2)^2}{r^2 - (a_1 - a_2)^2} \right\}, \quad (8)$$

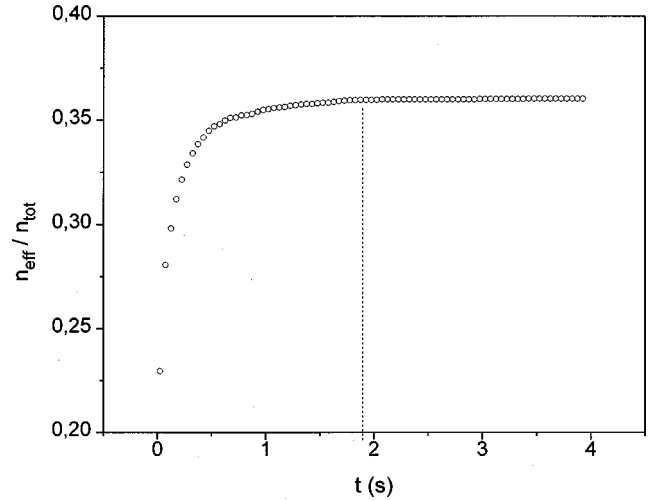


FIG. 1. Cumulative frequency plot of collision vs time. Initial distance: 500 nm. Average over 5000 random walks. No interaction between particles. $\Delta t = 2 \times 10^{-4}$ s.

$$V_E(r) = \epsilon \pi \frac{a_1 a_2}{a_1 + a_2} \{ (\psi_{01} + \psi_{02})^2 \ln(1 + e^{-\kappa(r - a_1 - a_2)}) + (\psi_{01} - \psi_{02})^2 \ln(1 - e^{-\kappa(r - a_1 - a_2)}) \}. \quad (9)$$

a_1 and a_2 are the particle radii, ψ_{01} and ψ_{02} are the surface potentials, r is the center to center distance, and κ is the Debye reciprocal length, which depends on the solvent ionic concentration.

The encounter probability between a Brownian particle and a fixed one is evaluated by simple counting after random paths were performed. When no encounter is detected in a reasonable time, the random path generation is forced to stop. In order to set this limiting time, t_{inf} , the occurrence of a collision was studied as a function of the aggregation time. Figure 1 shows a typical cumulative frequency graph, normalized to the total amount of random walks, generated using a time step of 2×10^{-4} s. It can be observed that almost all of the encounters take place in the first half-second. Therefore, in our simulations, we will use a step of 2×10^{-4} s and a $t_{\text{inf}} = 2$ s.

IV. MATERIAL AND METHODS

Two polymer latexes, with opposite sign surface charge densities have been used as colloidal systems. Negative and positive particles with similar sizes were synthesized as described in [24] and [25], respectively. Similarity in particle size makes interpretation of light scattering data easier and allows the use of simplifications for the HHF potentials. On the other hand, particle surface chemical groups produce a pH-dependent charge density that will be exploited to set similar electrical potentials on the particle surfaces. Table I shows the size and the critical coagulation concentrations (CCC) for both latexes. Since the CCC indicates the lowest ionic concentration that completely screens the particle charge, it has been widely used as a measure of the surface electric potentials. Similar CCC's were obtained for pH 4.5. Under these conditions the systems have similar particle size and stability, concluding that the surface electrical potentials

TABLE I. Particle sizes and critical coagulation concentration of both latexes at different pH's.

Name	D (nm) ^a	CCC (pH 11)	CCC (pH 4.5)	CCC (pH 3.5)
AM3	187±7	700±30 mM	185±25 mM	<10 mM
MP3	185±9	142±21 mM	213±24 mM	209±17 mM

^aDetermined by transmission electron microscopy.

are also similar (in absolute value).

Nonstandard use of a Malvern 4700 light scattering instrument has been made for monitoring aggregation processes. Slight modifications were performed for proper detection of the scattered intensity at short aggregation times from where the kinetic constants were determined. Special care was taken for increasing the amount of low dispersion data, which guarantees a proper measurement of such constants from the intensity-time curves.

Aggregations were carried out at an initial particle concentration of $N_0 = 2 \times 10^9 \text{ cm}^{-3}$ at $(25.0 \pm 0.1)^\circ \text{C}$. NaCl was used as 1:1 electrolyte for particle charge screening.

In homoaggregation, the dimer formation rate constant, k_{dim} was obtained from the initial slope by means of [26]

$$\frac{1}{I(q,0)} \left(\frac{dI(q,t)}{dt} \right)_{t=0} = \left(\frac{I_2(q)}{2I_1(q)} - 1 \right) k_{\text{dim}} N_0, \quad (10)$$

where I_n is the intensity scattered by a n -mer, where q is the scattering vector, $q = 4\pi/\lambda \sin \theta/2$, with λ the wavelength in the dispersive medium, and θ the scattering angle. Within the Rayleigh-Gans-Debye approximation, the optical factor $I_2(q)/[2I_1(q)]$, is given by [27]

$$\frac{I_2(q)}{2I_1(q)} = 1 + \frac{\sin 2qa}{2qa},$$

where a is the primary particle radius.

For heteroaggregation, Eq. (10) can be also employed to determine the rate constants, since the particles have the same radii. In this case, k_{dim} accounts for the three basic reactions: homocoagulation of each system and the pure heteroaggregation reaction. In order to obtain the contribution to dimer formation only from heteroaggregation, the following expression, developed by Hogg, Healy, and Fuerstenau [23] was used:

$$k_{\text{dim}} = n_1^2 k_{11} + n_2^2 k_{22} + 2n_1 n_2 k_{12}, \quad (11)$$

where n_i is the fraction of particles of type i and k_{ij} is the dimer formation rate constant for the reaction between particles of types i and j .

V. RESULTS AND DISCUSSION

Aggregation is the result of a competition between particle diffusion and the interaction thereof. Thus, two limiting behaviors become apparent when any of them dominates over the other, resulting in an aggregation totally controlled by diffusion of particles or a process mainly dominated by the interaction. By modifying the interaction between particles, the balance between these two limiting cases may be controlled.

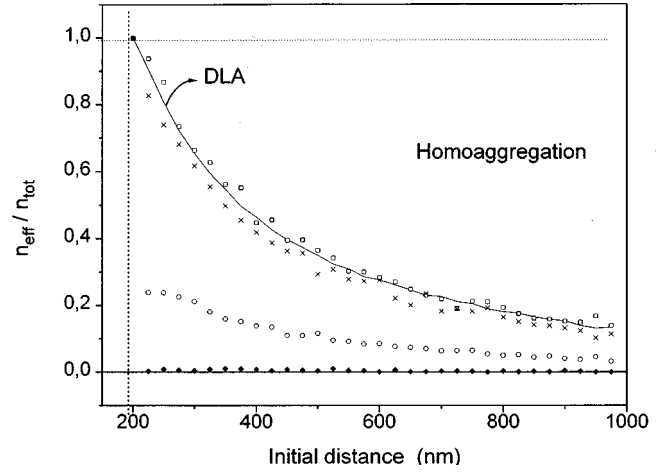


FIG. 2. Effect of initial distance and κ in homoaggregation. $\kappa = 5 \times 10^7 \text{ m}^{-1}$ (\blacklozenge), $\kappa = 10^8 \text{ m}^{-1}$ (\circ), $\kappa = 2.5 \times 10^8 \text{ m}^{-1}$ (\times) and $\kappa = 10^9 \text{ m}^{-1}$ (\square). Full line represents the values for DLA.

In this paper, the effect of strength and the range of the interaction on the aggregation probability will be studied. Two different electrical interactions, an attractive and a repulsive one, are used. Thus, homoaggregation and heteroaggregation processes are tackled. The encounter probability, $n_{\text{eff}}/n_{\text{tot}}$, where n_{eff} is the number of encounters and n_{tot} is the total number of random paths, has been used to study aggregation. In Fig. 2, the encounter probability is plotted as a function of the initial center to center distance for different values of the reciprocal Debye length κ . By varying κ , the strength of the interaction is controlled. In this simulation, both particles have the same radius and surface potentials, corresponding to a homocoagulation process. It should be noted that, in every case, the probability increases with increasing distance. For the lowest κ , the process is totally dominated by repulsive forces, and so the system is completely stable. As κ rises the interaction is screened and diffusion becomes more and more relevant, until the process is limited by diffusion [diffusion limited aggregation, (DLA)]. In this case, the value of κ has no effect (solid line in plot).

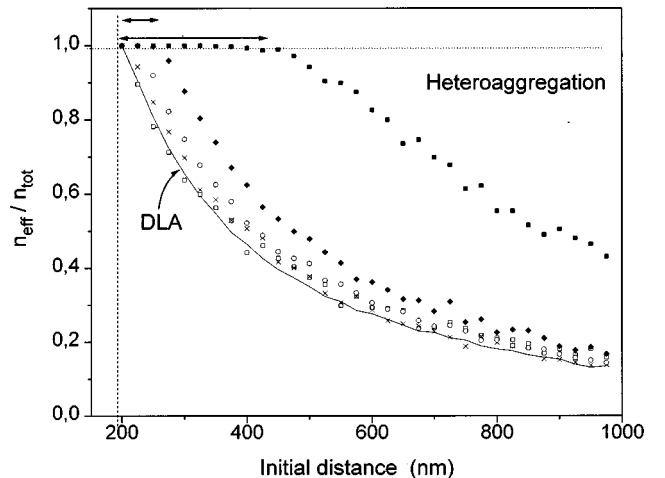


FIG. 3. Effect of initial distance and κ in heteroaggregation. $\kappa = 10^{-7} \text{ m}^{-1}$ (\blacksquare), $\kappa = 5 \times 10^7 \text{ m}^{-1}$ (\blacklozenge), $\kappa = 10^8 \text{ m}^{-1}$ (\circ), $\kappa = 2.5 \times 10^8 \text{ m}^{-1}$ (\times), and $\kappa = 10^9 \text{ m}^{-1}$ (\square). Full line represents the values for DLA.

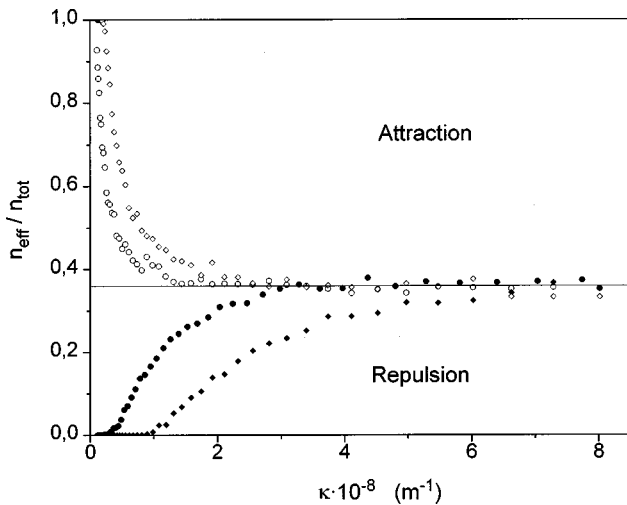


FIG. 4. Comparison of the effect of κ in homoaggregation (\bullet, \blacklozenge) and heteroaggregation (\circ, \diamond). Initial particle to particle distance: 500 nm. Full line represents the DLA value, for $|\phi_1| = |\phi_2| = 15$ mV (\bullet, \circ) and $|\phi_1| = |\phi_2| = 100$ mV (\blacklozenge, \diamond).

On the other hand, Fig. 3 shows results for heteroaggregation. For this purpose, two particles with similar radius but opposite surface electrical potential were considered. In contrast to homoaggregation, the attractive interaction is screened as κ rises, until diffusion plays the dominant role. It is interesting to point out that when the particles come closer than a critical distance, aggregation is guaranteed. The upper curve in Fig. 3, corresponding to the lowest κ , shows this feature. The encounter probability remains constant and equal to one, up to a certain value, beyond which it decays. This critical distance can be interpreted as a measure of the competition between diffusion and attraction. This fact can be confirmed in Fig. 3, where the critical distance reduces for increasing κ (which implies attraction screening). In the limit $\kappa \rightarrow 0$ the critical distance tends to infinity, and an attraction limited aggregation regime (ALA) could be defined. In this sense, heteroaggregation curves appearing in Fig. 3, are interpreted as intermediate regimes between DLA and ALA.

In order to study the crossing from ALA to DLA, the encounter probabilities were calculated as a function of the Debye reciprocal length (Fig. 4). Furthermore, this plot will be compared with experimental results. For homoaggregation the system is highly stable for low κ , and tends to DLA as κ rises. In contrast, for heteroaggregation, processes faster than DLA are found. At low ionic concentration, the probability tends to 1, where all trials are effective (ALA), and slows down as κ increases. Therefore, the aggregation mechanism crosses from ALA to DLA. Furthermore, the DLA limit is reached for a lower κ value than in homoaggregation. These trends are observed independently of the

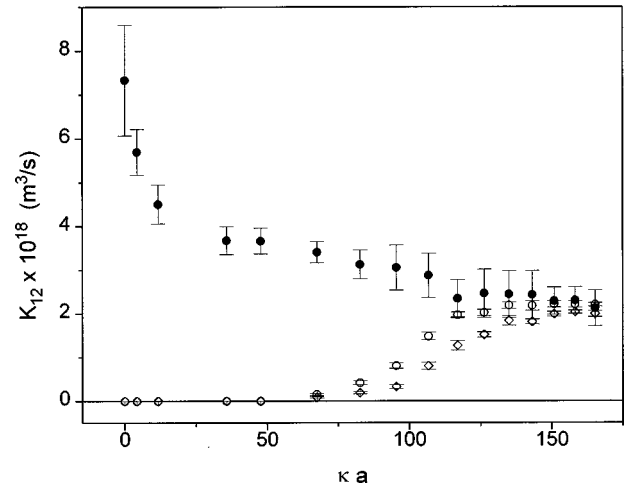


FIG. 5. Dimer formation rate constant. Heteroaggregation (\bullet), homoaggregation of latex AM3 (\circ), and homoaggregation of latex MP3 (\diamond).

surface potentials used in simulations (Fig. 4), which indicates that the results are only related to the nature of the interactions.

Experiments were performed for testing these findings. Experimental conditions were set to ensure similar surface potentials, to be compared with simulations. The doublet formation rate constants were determined for homoaggregations and heteroaggregations by static light scattering, as described in Sec. IV. Figure 5 shows the kinetic constant for different values of κ . At high salt concentration both homo and heteroaggregation tend to the same value, which is typical for DLA [4]. As electrolyte concentration decreases, homoaggregation becomes slower and slower, until the system is stable. In contrast, for heteroaggregation the process speeds up as salt concentration is decreased, reaching values for the kinetic constant several times larger than the DLA value. These results are in good agreement with those reported in literature at very low salt concentrations [7,8,10]. Thus, the transition from processes controlled by attraction forces to diffusive aggregation has been experimentally accessed.

It is interesting to emphasize the identical behaviors clearly observed from comparison between experimental curves and simulations. This fact validates the model for describing early stages of homoaggregation and heteroaggregation, when only dimers are growing.

ACKNOWLEDGMENTS

The financial support provided by CICYT (under Project No. MAT-96-1035C03-03) is greatly appreciated. A. Puertas thanks the University of Almería for funding. The authors are also grateful to M. S. Romero-Cano for synthesizing the latexes used throughout this work.

[1] M. von Smoluchowski, Z. Phys. Chem., Stoechiom. Verwandtschaftsl. **92**, 129 (1917).

[2] R. M. Ziff, M. H. Ernst, and E. M. Herdriks, J. Phys. A **16**, 2293 (1983).

[3] F. Family and D. P. Landau, *Kinetics of Aggregation and Gelation* (Elsevier, Amsterdam, 1984).

[4] H. Sontag, K. Strenge, *Coagulation Kinetics and Structure Formation* (Plenum, New York, 1987).

- [5] H. Kihira, N. Ryde, and E. Matijević, *Colloids Surface* **64**, 317 (1992).
- [6] H. Kihira, N. Ryde, and E. Matijević, *J. Chem. Soc., Faraday Trans.* **88**, 2379 (1992).
- [7] H. Kihira and E. Matijević, *Langmuir* **8**, 2855 (1992).
- [8] N. Ryde and E. Matijević, *J. Chem. Soc., Faraday Trans.* **90**, 167 (1994).
- [9] A. M. Islam, B. Z. Chowdhry, and M. J. Snowden, *Adv. Colloid Interface Sci.* **62**, 109 (1995).
- [10] J. A. Maroto and F. J. de las Nieves, *Colloids Surf., A* **96**, 121 (1995).
- [11] M. D. Haw, M. Sievwright, W. C. K. Poon, and P. N. Pusey, *Adv. Colloid Interface Sci.* **62**, 1 (1995).
- [12] F. Family, P. Meakin, and T. Vicsek, *J. Chem. Phys.* **83**, 4144 (1985).
- [13] T. Vicsek, *Fractal Growth Phenomena* (World Scientific, Singapore, 1992).
- [14] J. H. J. van Opheusden, M. T. A. Bos, and G. van der Kaaden, *Physica A* **227**, 183 (1996).
- [15] M. T. A. Bos and J. H. J. van Opheusden, *Phys. Rev. E* **53**, 5044 (1996).
- [16] M. Whittle, E. Dickinson, *Mol. Phys.* **90**, 739 (1997).
- [17] J. K. G. Dhont, *An Introduction to Dynamics of Colloids* (Elsevier, Amsterdam, 1996).
- [18] S. Chandrasekhar, *Rev. Mod. Phys.* **15**, 1 (1943).
- [19] W. H. Press, S. A. Teukolsky, W. T. Vetterling, and B. P. Flannery, *Numerical Recipes in C* (Cambridge University Press, New York, 1992).
- [20] B. J. T. Morgan, *Elements of Simulation and Monte Carlo Method* (Chapman and Hall, London, 1984).
- [21] B. V. Derjaguin and L. D. Landau, *Acta Physicochim. URSS* **14**, 733 (1941).
- [22] E. J. W. Verwey and J. Th. G. Overbeek, *Theory of Stability of Lyophobic Colloids* (Elsevier, Amsterdam, 1948).
- [23] R. Hogg, T. W. Healy, and D. W. Fuerstenau, *J. Chem. Soc., Faraday Trans.* **62**, 1638 (1966).
- [24] R. Hidalgo-Alvarez, F. J. de las Nieves, A. J. van der Linde, and B. H. Bijsterbosch, *Colloids Surface* **21**, 259 (1986).
- [25] D. Bastos, J. L. Ortega, F. J. de las Nieves, and R. Hidalgo-Alvarez, *J. Colloid Interface Sci.* **176**, 232 (1996).
- [26] D. Giles and A. Lips, *J. Chem. Soc., Faraday Trans.* **74**, 733 (1978).
- [27] M. Kerker, *The Scattering of Light and other Electromagnetic Radiation* (Academic, New York, 1969).